Ceramics International **21** (1995) 325–333

The Injection Moulding of Fine and Ultra-fine Zirconia Powders

J. H. Song & J. R. G. Evans

Department of Materials Technology, Brunel University, Uxbridge, Middlesex, UB8 3PH, UK

(Received 16 November 1994; accepted 29 January 1995)

Abstract: Injection moulded components and test bars were prepared from three zirconia powders with specific surface areas of 22, 7 and 4 $m^2 g^{-1}$ at 50–60 vol% ceramic. The organic vehicle was a microcrystalline wax with a large addition of dispersant, either in the form of stearic acid or a proprietary polyester. The flexural strengths of the bars were recorded and the critical defects identified by fractography.

1 INTRODUCTION

The thermodynamic and kinetic considerations of ceramic sintering processes are stimulating the production of chemically derived powders in the <100 nm region. The restriction on grain size of metastable tetragonal zirconia, which is about 1 μm, also requires a starting powder which is fine and of narrow size distribution. If ceramic injection moulding is to be accepted as a mainstream powder assembly process, it must be able to operate with a wide range of powders, including the ultra-fine.

There are many examples of the injection moulding of relatively coarse (>1 μm) powders,[1] but few reports of ultra-fine powder injection moulding. The traditional view is that fine powders can be incorporated in organic vehicles only at low loadings (<50 vol%). Recent work has shown that provided attention is given to the type of dispersant, high volume fractions (>60 vol%) can be processed.[2] The second problem is that all the mass transport processes associated with binder removal are impeded by the use of fine powders.[3] In this study, two ultra-fine and one somewhat coarser ZrO_2 powders of approximately the same chemical composition were injection moulded using similar organic vehicles and the products were examined for defects by microscopy and flexural strength testing.

2 EXPERIMENTAL DETAILS

2.1 Materials

The details of the ceramic powders and organic materials selected are given in Table 1. Powders Z4 and Z5 are experimental grades of ultra-fine zirconia whose BET specific surface areas are partly due to the porosity of an inorganic coating. They have been spray dried. Powder Z6 is a commercially available powder, apparently without such a coating and is not in a spray dried state. Powder PSZ–Y5 is an electrofused zirconia which has been subject to mechanical comminution and has irregular particle shape.

The microcrystalline wax has been used as a base for organic vehicles for ceramic injection moulding in many reports, partly because it presents a steady weight loss on pyrolysis.[4] Stearic acid is frequently selected as a lubricant/dispersant; its precise role being ill-defined. Hypermer KD5 is one member of a class of proprietary dispersants,[5] being itself specially recommended for dispersion of ceramics in non-polar media. Table 2 shows the composition of mixtures prepared for injection moulding. The organic vehicles are based on extensive study of viscosity,[2] flocculation[6] and phase separation.[7]

2.2 Mixing

The powders were dried in a vacuum oven at 110°C for 24 h before mixing. Pre-mixing was

Ceramics International Printed in Great Britain

Table 1. Details of materials

Type	Grade	Source	Density (kgm^{-3})	Y_2O_3 content (wt%)	Average particle size (nm)	Specific surface area ($m^2 g^{-1}$)
Zirconia	Z4/Z5[a]	Tioxide Specialties, UK	5579[b]	4·5–5·0	70	22
Zirconia	Z6	—	6000	5·0	100	7
Zirconia	PSZ–Y5	Unitec Ceramics, UK	6000[c]	5·0	1500 (1·5 μm)	4
Micro-crystalline wax	Okerin 1865H	Astor Chemicals, UK	905	—	—	
Stearic acid	GPR	BDH-Merck, UK	941	—	—	—
Dispersant	Hypermer KD5	ICI Surfactants, UK	910	—	—	—

[a]Z4 and Z5 are formally identical but emerge from different batches. Powder Z5 is made up of similar constituents from three separate batch numbers.
[b]Calculated from compositions based on mixed oxides and checked by helium pycnometry.
[c]Manufacturers information.

Table 2. Compositions of suspensions used for injection moulding (calculated from loss on ignition)

	Composition (wt%)					
Component	A	B	C	D	E	F
Z4	—	88·25	90·21	—	—	—
Z5	85·80	—	—	—	—	—
Z6	—	—	—	88·89	90·85	—
PSZ–Y5	—	—	—	—	—	90·80
Wax	7·10	5·29	4·41	7·22	5·95	5·98
Stearic acid	7·10	—	—	3·89	—	3·22
Hypermer KD5	—	6·46	5·38	—	3·20	—
Vol% ceramic	50	55	60	55	60	60

carried out by stirring powder into molten wax and dispersant. Compounding was carried out on a twin screw extruder (Model TS40, Betol Machinery, Luton, Bedfordshire, UK). The barrel temperatures were 70–80–100–110°C feed to exit and the screw rotation speed was 50–80 rpm. The mixtures were granulated and remixed to obtain greater homogeneity.

2.3 Moulding

The granulated mixtures were dried in a vacuum oven at 70°C for 24 h before injection moulding using a Negri Bossi NB90 machine (John Brown Plastics Machinery, Chesterfield, UK). Bars suitable for flexural strength testing, 6 × 10 × 89 mm, and gear wheels, 29 mm o.d., were produced by conventional injection moulding. The barrel temperatures were generally 60–70–80–90°C feed–nozzle, although the nozzle and adjacent barrel sections were raised to 110°C to mould the PSZ–Y5 powder at 60 vol%. The mould temperature was 40–46°C throughout. Injection pressures were 10–50 MPa and hold pressures were 5–25 MPa. A second stage pressure trip mechanism was used. The screw rotation speed was 80 rpm and injection rate was 2–5 × 10^{-5} m^3 s^{-1}.

2.4 Pyrolysis and sintering

Removal of organic vehicle was carried out by controlled heating in oxygen-free nitrogen. The samples were supported in an alumina setter powder (LG20 ex Alcan Chemicals, UK) to prevent slumping and to assist in partitioning of molten wax. The bars made from the fine powders were heated at 30°C/h to 90°C, and thereafter at 2°C/h to 480°C and furnace cooled. Bars made from the coarse powder were heated at 5°C/h to 450°C and furnace cooled. All the gear wheels were heated at 4°C/h to 450°C. In some experiments the nitrogen was allowed to flow through water before entering the furnace.

Sintering was carried out in air in a tube furnace (Isoheat, Worksop, UK). For the fine powders and some coarse powder mouldings a heating ramp of 1°C/min to 1450°C with a 1 h dwell was used. Some of the coarse powder mouldings were sintered at 1525°C for 2 h, as recommended by the powder manufacturer. Linear shrinkage after

binder removal and sintering was measured with a travelling microscope. Densities of sintered bars were measured by the Archimedes method (ANSI/ASTM A/D 792-66).

2.5 Mechanical testing

The sintered bars were tested in three point loading on a model 4206 Instron machine (High Wycombe, Bucks, UK) with a cross head speed of $8{\cdot}3 \times 10^{-6}$ ms^{-1} and a span of 55 mm. The average section dimensions of the bars were 8 mm × 4·5 mm in depth, depending on sintering conditions and initial volume fraction. Some bars were diamond ground and polished on 6 μm grade diamond paste before testing. These were tested with a span of 29 mm so that two samples could be tested from each bar and the bars were smaller in section (3·8 mm × 7·1 mm). A slight volume effect will arise from these changes. Fracture surfaces were observed in a scanning electron microscope (Camscan S250, Cambridge Scientific Instruments).

3 RESULTS AND DISCUSSION

3.1 Injection moulding

The mixtures given in Table 2 were devised after a systematic study of the particular problems associated with injection moulding of ultra-fine zirconia. The powders are shown in Fig. 1. Powders Z4 and Z5 have ultimate particular sizes of about 70 nm on average, while Z6 has an average particle size of 100 nm. In contrast, PSZ–Y5 has a mean particle size of 1·5 μm, with a much wider distribution and a maximum size <5 μm.

Fine powders may adsorb substantial water which could cause problems during subsequent heat treatment of mouldings.[3] Although the powders were dried as a matter of routine before mixing, this was not very effective. The weight loss from thermogravimetric analysis of powder was 0·2 wt% for PSZ–Y5, whether it had been vacuum dried or not. For Z4, the weight loss was 1·6 wt% for the powder as received, and 1·3 wt% after drying. The powders are likely to be powerful dessicants and to re-adsorb moisture rapidly after drying.

It has been shown that when fine powders are incorporated in organic fluids, relative viscosities, η_r, are very high.[2] Thus in a polymeric vehicle, the volume loading is restricted by the resulting apparent viscosity of the suspensions η, which is related to the apparent viscosity of the unfilled system by $\eta = \eta_r \eta_o$. A low viscosity wax-based system was therefore selected.

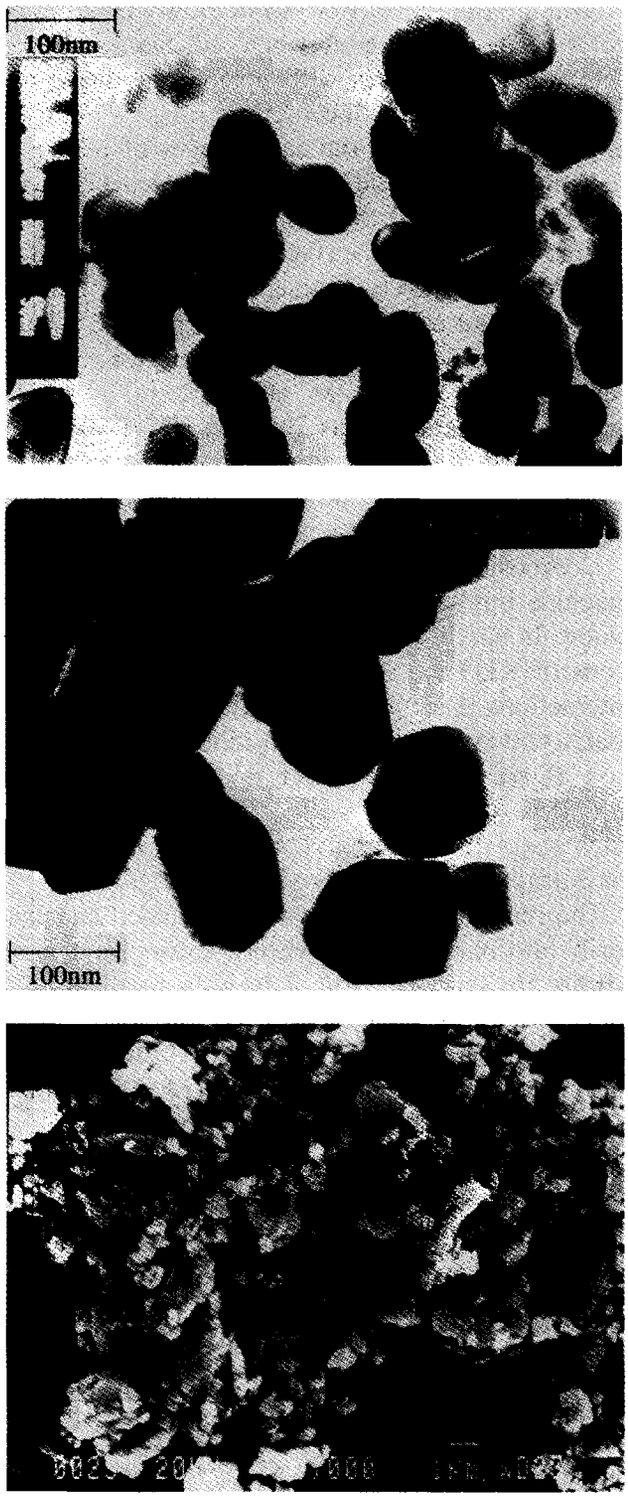

Fig. 1. Scanning electron micrographs of the zirconia powder. (a) Z4, (b) Z6 and (c) PSZ–Y5.

It has been shown that without a stabilizing additive, the fine powders could be incorporated into wax at a maximum of 32 vol%.[2] This mixture failed to pass the capillary rheometer die and could not be moulded. Stearic acid and the proprietary KD5 were selected as dispersants. The latter is a polyester with molecular weight of about 750 and is synthesised to give stabilization in non-polar liquids.

Volume fractions of ultra-fine powders up to 60 vol% became mouldable when sufficient stabilizer was added.[2] Mixtures with insufficient dispersant were found to show flocculation, phase separation and cracking during the early stages of reheating to remove the vehicle.[6,7] Stability is dependent on surface coverage of the powder and thus is closely related to specific surface area.[8] The powder PSZ–Y5 is relatively coarse, with a wide particle size distribution and irregular particle shape resulting from mechanical comminution. It was very easy to mould at 60 vol% in a stearic acid–wax system, but at 70 vol% (KD5–wax system) caused machine seizure. Thus, both relatively coarse and ultra-fine powders could be moulded at 60 vol% (Table 2).

Composition B was introduced to the moulding machine but satisfactory mouldings could not be made. It has been reported previously that additions of KD5 are so effective in reducing particle interactions that mouldings with low zirconia contents (<50 vol%) slump when reheated.[8] Composition B was extremely soft and sticky and this inhibited the proper mode of flow at the screw-back stage of moulding. This resulted in extensive air entrapment and all mouldings were scrap.

The remaining mixtures were moulded satisfactorily into bars and gear wheels. Examples of gear wheels are shown in Fig. 2 in both moulded and sintered states. Figure 3 shows the rectangular bars in the moulded and sintered form. Some of the moulded gear wheels showed weld lines projecting from the corners of the square recess. Although this results from a gating design fault in the cavity it could be removed by the use of higher injection pressure and speed.

3.2 Pyrolysis and sintering

Failure to achieve sufficient flow rate of nitrogen to the pyrolysis oven or to water cool the furnace end caps resulted in discolouration of the mouldings with carbon residue. The minimum flow rate was 5×10^{-7} m^3 s^{-1} for 100 g of mouldings and condensed wax could be collected from the furnace end caps. When these precautions were not observed, opening the furnace and exposing discoloured mouldings to ambient air caused audible and visible cracking and spalling. The formation of a carbon deposit in an organic binder, which should be lost mainly by evaporation,[9] is likely to be caused by chemical cracking of the hydrocarbon on the active zirconia surface under conditions where a high partial pressure of wax exists in the furnace. The effect of the damage was alleviated by passing the nitrogen through water on entry; an intervention that is suggested by the fact that sudden exposure to a wet atmosphere after drying to 450°C may cause expansion of the powder with active carbon residue.[10]

The shrinkage associated with binder removal is shown in Table 3. The Z6 mouldings show a slight expansion but the error associated with this measurement was about 0·5%. In contrast, the Z4 and Z5 powders show the expected shrinkage pattern,[11] with a higher shrinkage for suspensions of initially lower volume fraction. The PSZ–Y5 mouldings show almost no shrinkage and it can be concluded that at 60 vol% the powder is close

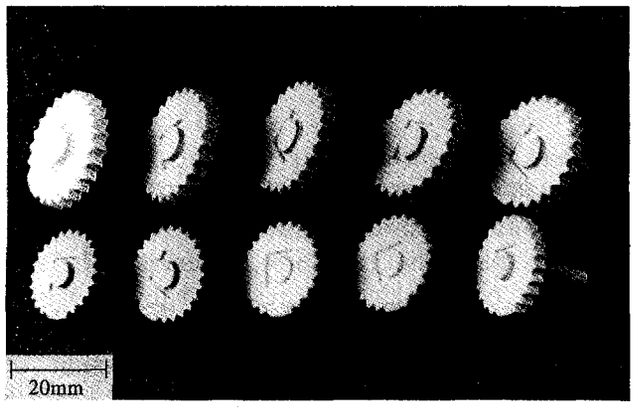

Fig. 2. Moulded and sintered gears.

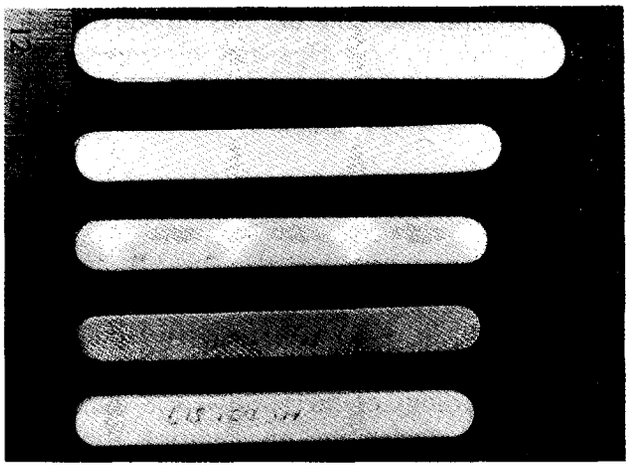

Fig. 3. Moulded and sintered rectangular bars.

Table 3. Shrinkage or dilation of bars caused by removal of the organic vehicle

Moulding compositions	Change in length (%)		
	Length	Width	Thickness
D	+0·5	+0·3	+0·6
E	+0·2	+0·4	+0·5
A	−4·5	−4·3	−4·2
C	−3·5	−3·6	−3·7
F	−0·1	−0·4	+0·4

Table 4. Linear shrinkage on sintering

Moulding composition	Linear shrinkage (%) Length	Width	Thickness	Initial relative density (%)	Final density (kgm^{-3})	Final relative density (%) (i)	(ii)
D	18·3	18·4	18·2	55	6021	99·5	100
E	15·6	15·6	15·8	60	6043	99·9	99·2
A	18·5	18·9	19·2	57	5931	97·2	97·6
C	14·3	15·1	14·8	67	5903	96·8	98·8
F (1450°C)[a]	12·4	14·9	14·6	60	—	—	92·6
F (1525°C)[a]	11·5	15·4	15·4	60	5733	94·0	93·2

[a]Sintering temperature.
(i) Calculated from measured density.
(ii) Calculated from volume fraction, shrinkage and changes in theoretical density.

to its maximum packing efficiency. This is consistent with the seizure of the moulding machine caused by higher loadings.

The failure of the 50 vol% and 60 vol% Z6 mouldings to show shrinkage on binder removal is perplexing. It is shown below that a high proportion of the Z6 mouldings showed central longitudinal cracks after sintering. These arose during binder removal but were not visible in the fracture surface after moulding. Correct shrinkage measurements cannot be performed on mouldings which have cracked. This does not, however, explain the absence of shrinkage in the longitudinal direction.

Table 4 shows the shrinkage on sintering and the final densities. The initial relative density is calculated from the ceramic volume loading deduced by loss on ignition and the shrinkage on binder removal shown in Table 3. Table 4 also shows the final relative densities calculated from measured densities and these compare favourably with the same quantity calculated from initial ceramic volume fraction, shrinkage on pyrolysis, shrinkage on sintering and changes in theoretical density between powder and sintered body. The modest sintering schedules have provided reasonable final densities and inspection of fracture surfaces for Z4 and Z5 sintered mouldings showed maximum grain sizes of about 0·5 μm. Thus some additional grain growth can be tolerated in bringing the final density up.

Since it is known that the ultra-fine powder does not fully disperse in wax-based systems, density measurements were carried out on fragments of mouldings to check for occluded gas. The density of composition A was 3295 kgm^{-3}, slightly higher than the theoretical value based on the mixture which was 3250 kgm^{-3}. Similarly, the density of composition C was 3732 kgm^{-3}, compared with a theoretical value of 3710 kgm^{-3}. The discrepancy can be accounted for by conformational differences in the organic molecules in the presence of high energy surfaces and they suggest that occluded gas is absent.

3.3 Mechanical tests and identification of critical defects

A wide distribution of three point flexural strengths was recorded from bars fabricated from all three powders and these strengths corresponded to injection moulding defects rather than intrinsic properties of the powders. The results are summarized in Table 5. The highest strength recorded from unmachined mouldings of composition C was 584 MPa, while powder Z6 gave 483

Table 5. Summary of three point flexural strength testing of injection moulded and sintered bars

Powder	Injection moulding composition (Table 2)	Mean strength (MPa)	Standard deviation (MPa)	No. of tests	Max. strength (MPa)	Min. strength (MPa)
Z6	E	267	55	20	361	1
Z6	D	300	92	20	483	1
Z6	E (polished surface)	659	212	5	873	3
Z6	D (polished surface)	661	208	7	895	3
PSZ–Y5	F	287	114	10	496	1
Z4	C	315	153	11	584	85
Z5	B	96	76	5	215	20
Z4	C (polished surface)	518	85	3	575	4

MPa, and the relatively coarse PSZ–Y5 gave 496 MPa maximum. For the ultra-fine powders these strengths are about half those recorded from components fabricated by compaction under clean conditions. Superifically therefore, the critical defects should be about four times as large. This assumes that the critical defects are distributed uniformly throughout the body and this is not the case for injection moulding defects, which tend to be preferentially located near the centre of mouldings and hence near the neutral axis in flexural testing. Because many different defect types are present, the distribution of strength cannot be assessed by the Weibull distribution, which assumes a single population. It follows that fractography gives much more useful information about the nature and size of critical defects than does the flexural strength.

In the captions to the fractographs shown below, a value for the critical defect size C, has been calculated from Griffith's equation:

$$C = \left(\frac{Z.K_{IC}}{y\ \sigma_f} \right)^2$$

assuming that $Z = \pi/2$ for a semicircular crack and that the compliance function $y = 2$ for a defect at the edge of the tensile face and for which $C << W$, where W is the thickness of the bar. For defects situated near the centre this gives a meaningless value of C. The fracture toughness was taken as 8 $MPam^{1/2}$.

Figure 4 shows a fracture surface of a Z6 bar in low magnification which was typical of many of the test bars. Fracture surface striations direct attention to the lower left corner where the initiating defect is seen (Fig. 5). This micrograph shows the deeply pitted surface which was typical of all the mouldings and accounts for most of the low strengths. Because the authors were concerned to

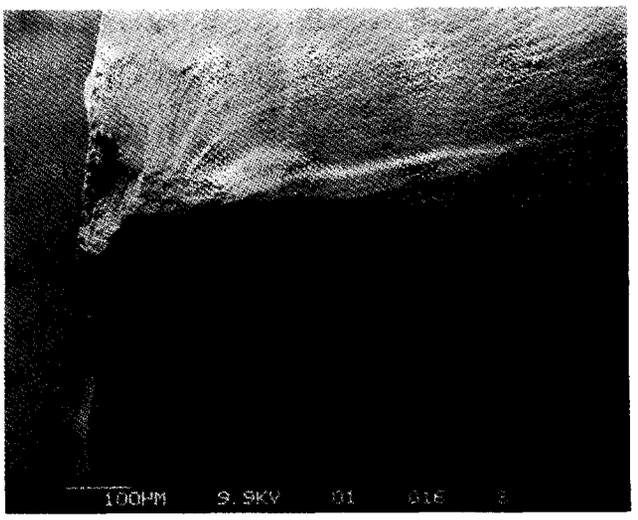

Fig. 5. The corner of the bar shown in Fig. 4 showing the fracture-initiating defect.

avoid the shrinkage-related defects typical of injection moulded ceramics they had produced a high ceramic volume fraction suspension for an ultra-fine powder, used a low injection temperature and a low injection pressure compatible with mould filling. The 'crocodile skin' surface texture is produced on mould filling and is a function of these three parameters, as well as injection speed. It is related to the rheological properties at the mould wall where the shear rate experienced by the material is highest and chilling is rapid on mould entry. The roughness is on a scale that produces a matt appearance to the eye, but its implications for mechanical properties were not appreciated at the time of moulding.

The effect is shown in more detail in Fig. 6, which shows the edge of a fracture surface of a bar of composition E, wherein the ceramic loading is higher than that in Figs 4 and 5. The intrusion of the folds into the bulk is enhanced at the cor-

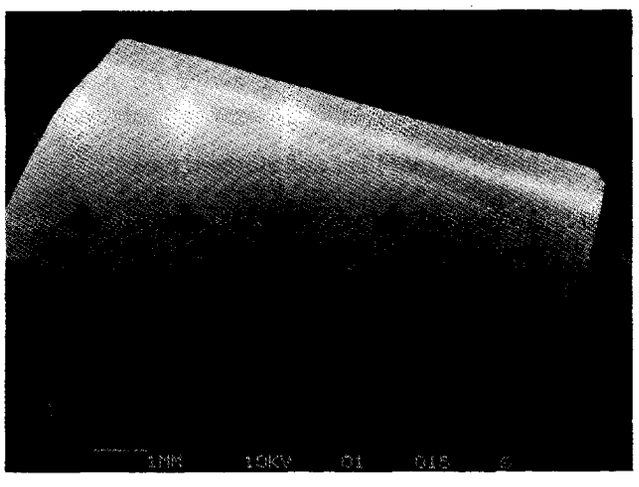

Fig. 4. Fracture surface of a bar made from composition D which gave a flexural strength of 322 MPa (C = 380 μm).

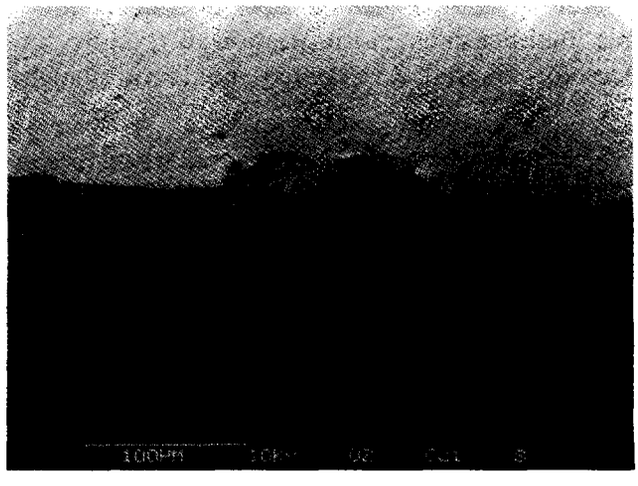

Fig. 6. The edge of the fracture face of a bar made from composition E showing the 'crocodile skin' caused on moulding filling.

ners of mouldings where chilling of the fluid is more rapid and many fractures, like that in Fig. 4 originated at the corners. Their effect serves to show that even in a low viscosity wax, if high volume fraction of ceramic is desired, high injection pressures and/or speed are needed.

The somewhat coarser powder PSZ–Y5 also tended to fracture from corner defects, although the 'crocodile skin' effect was less severe. Some moulded bars had central cracks arising from particle movements during thermolysis of the wax. Figure 7 shows such a crack in a bar which gave a strength of 424 MPa. Figure 8 shows the fracture face at higher magnification and reveals the residual porosity corresponding to the low relative density quoted in Table 4. The toughness of this material is not known and so no critical defect size was calculated.

A high proportion of the fracture surfaces investigated had surface defects similar to those shown in Fig. 9. These seem to be associated with the 'crocodile skin' effect when folding of the molten suspension has occurred during mould filling.

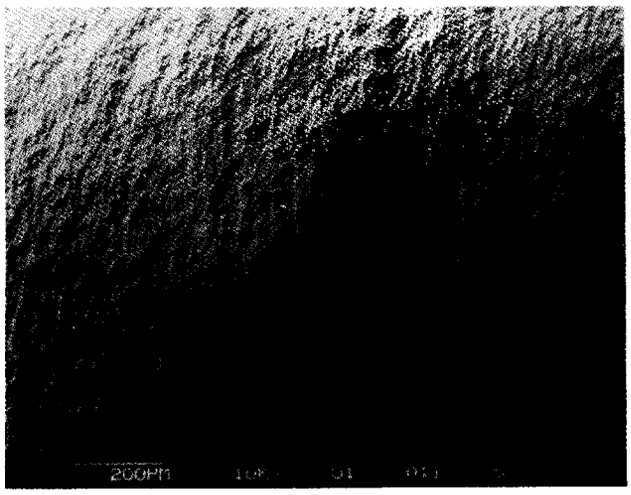

Fig. 7. Central crack in a bar of composition F. (flexural strength 424 MPa).

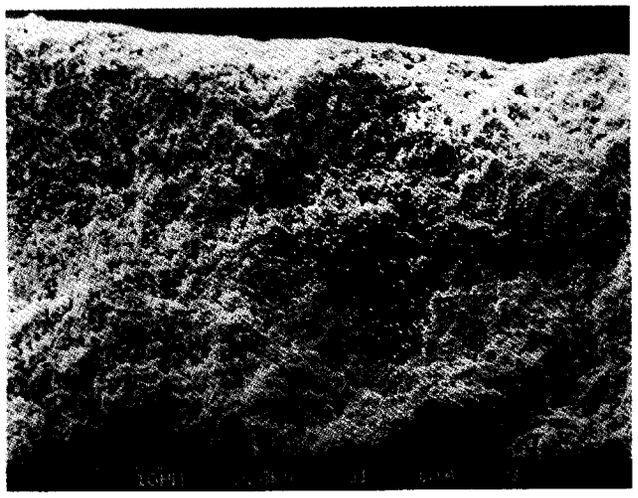

Fig. 8. Fracture face of a bar of composition F showing residual porosity.

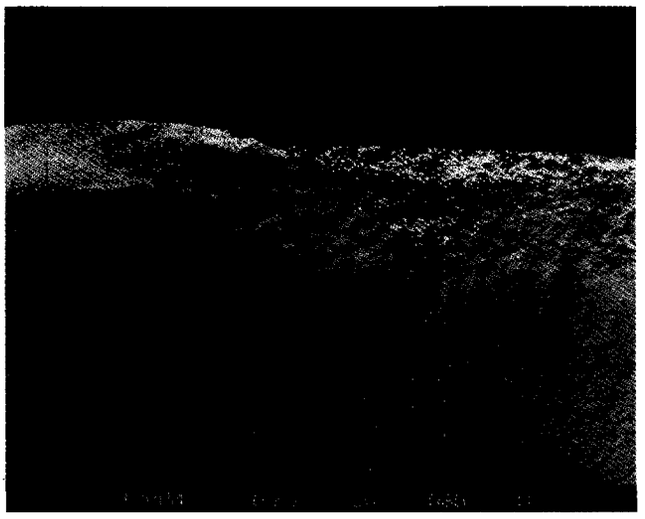

Fig. 9. A surface defect in a bar of composition D (flexural strength 341 MPa, C = 340 μm).

The highest strength obtained from moulded bars of powder Z4 was 584 MPa. Figure 10 shows the fracture face of this bar. It has a large pore caused by shrinkage on solidification and central cracks running along the length of the bar which arose from particle movements during binder removal. The high strength reflects the fact that the surface of these mouldings was somewhat better. This fracture face provides a good illustration of the blindness of strength measurements unsupported by fractography. The predominant surface defect shown in Figs 5, 6, 9 and 11 was removed from some bars by diamond grinding, followed by polishing on a 6 μm diamond wheel. The strengths obtained from these bars, as shown in

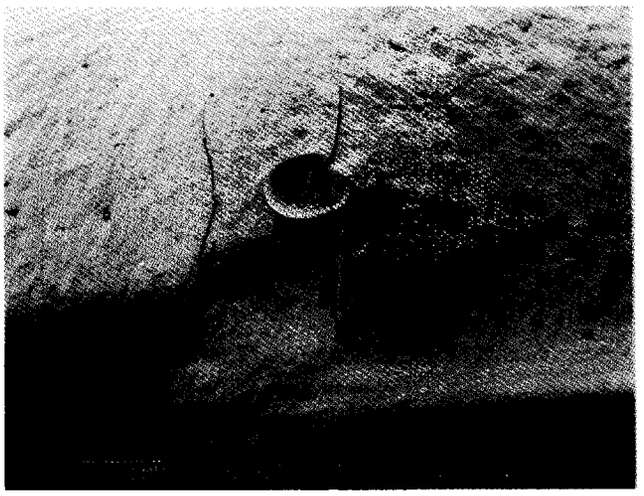

Fig. 10. Fracture face of a bar made from composition A (flexural strength 548 MPa, C = 115 μm).

Fig. 11. Combined surface defect and pore as initiation sites for fracture of a bar of composition C (flexural strength 369 MPa, C = 290 μm).

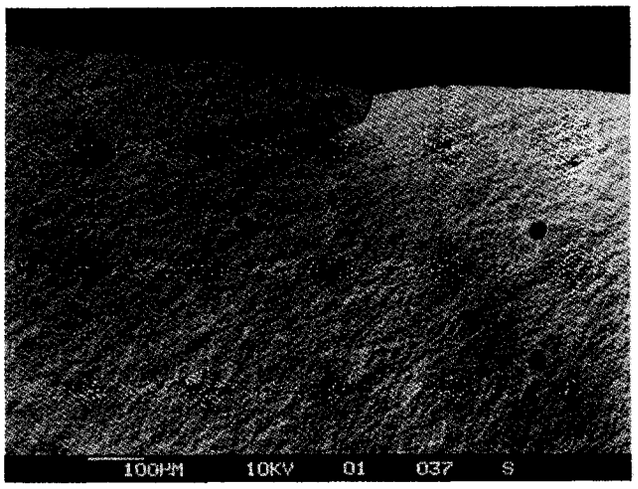

Fig. 12. Fracture initiation from a surface crack in composition C (flexural strength 219 MPa). Porosity in the 1–20 μm region can be detected.

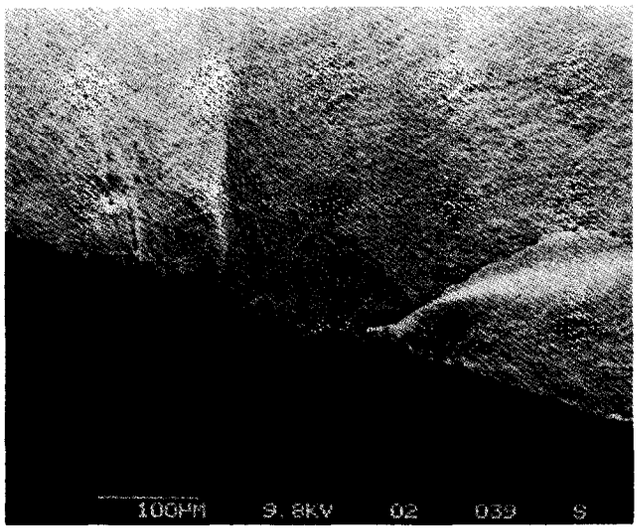

Fig. 13. Fracture initiation from surface defects in composition C (flexural strength 254 MPa).

Table 5, are considerably higher and approach the 1 GPa typical of compacted powders of this type. The remaining (volume distributed) defects are all attributable to injection moulding or contamination during processing.

4 CONCLUSIONS

By tailoring the composition of organic vehicle to suit high surface area ultra-fine zirconia powder, compositions containing 60 vol% ceramic could be injection moulded. Many of the shrinkage-related defects characteristic of injection moulding were avoided by the use of low injection pressure and barrel temperature, but this produced a 'crocodile skin' surface defect not previously reported. This reduced the measured strength to about half the value that would be obtained from similar powders assembled by compaction processes. However, inspection of the fracture surfaces failed to reveal evidence of the inter-agglomerate flaws characteristic of compacted assemblies.

ACKNOWLEDGEMENTS

The authors are grateful to the Science and Engineering Research Council for funding this work as part of the Link Nanotechnology Initiative. Ian Birkby, of Dynamic Ceramic, kindly donated the mould tool and carried out diamond machining. Dr G. Dransfield of Tioxide Specialties, UK, kindly donated the experimental zirconia. Mrs K. Goddard is thanked for typing the manuscript.

REFERENCES

1. EDIRISINGHE, M. J. & EVANS, J. R. G., Review: Fabrication of engineering ceramics by injection moulding I. Materials selection. *Int. J. High Tech. Ceramics*, **2** (1986) 1–31.
2. SONG, J. H. & EVANS, J. R. G., The role of dispersants in the rheological behaviour of ultrafine ceramic powder suspensions. (Submitted).
3. EVANS, J. R. G. & EDIRISINGHE, M. J., Interfacial factors affecting the incidence of defects in ceramic mouldings. *J. Mater. Sci.*, **26** (1991) 2081–88.
4. STEDMAN, S. J., EVANS, J. R. G. & WOODTHORPE, J., A method for selecting organic materials for ceramic injection moulding. *Ceram. Int.*, **16** (1990) 107–13.
5. SCHOFIELD, J. D., In *Recent Developments in the Technology of Surfactants*, ed. M. R. Porter. Elsevier, London, 1990, pp. 35–63.
6. SONG, J. H. & EVANS, J. R. G., Flocculation after injection moulding in ceramic suspensions. *J. Mater. Res.*, **9** (1994) 2386–97.
7. SONG, J. H. & EVANS, J. R. G., Phase separation during the reheating of ceramic mouldings. *Processing of Advanced Materials*, **3** (1993) 193–98.
8. SONG, J. H. & EVANS, J. R. G., Surface coverage of dispersants and deflocculation of ultrafine ceramic suspensions. (Submitted).

9. WRIGHT, J. K., EVANS, J. R. G. & EDIRISINGHE, M. J., Degradation of polyolefin blends used for ceramic injection moulding. *J. Amer. Ceram. Soc.*, **72** (1989) 1822–28.
10. DACEY J. R., Active carbon. In *The Solid Gas Interface*, Vol. 2, ed. E. A. Flood. Arnold, London, 1967, pp. 995–1022.
11. WRIGHT, J. K., EDIRISINGHE, M. J., ZHANG, J. G. & EVANS, J. R. G., Particle packing in ceramic injection moulding. *J. Amer. Ceram. Soc.*, **73** (1990) 2653–58.